

Modelling airborne transmission of SARS-CoV-2 using CARA: Risk assessment for enclosed spaces

Supplementary Material

S.I Equations

The total deposition fraction, f_{dep} , as a function of particle diameter D , is, according to Hinds [1]:

$$f_{\text{dep}}(D) = I_{\text{frac}}(D) \left(0.0587 + \frac{0.911}{1 + e^{4.77 + 1.485 \cdot \ln D_{\text{evap}}}} + \frac{0.943}{1 + e^{0.508 - 2.58 \cdot \ln D_{\text{evap}}}} \right), \quad (\text{Eq S.1})$$

with

$$I_{\text{frac}}(D) = 1 - 0.5 \left(1 - \frac{1}{1 + 0.00076 \cdot D_{\text{evap}}^{2.8}} \right),$$

and $D_{\text{evap}} = f_{\text{evap}} \cdot D$ (with $f_{\text{evap}} = 0.3$, D in μm).

S.II Figures

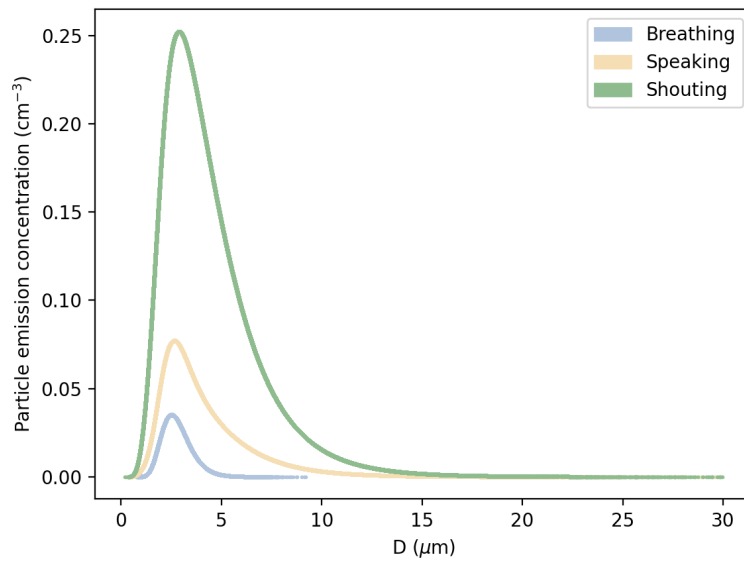


Figure S. 1: Particle emission concentration as a function of it's diameter.

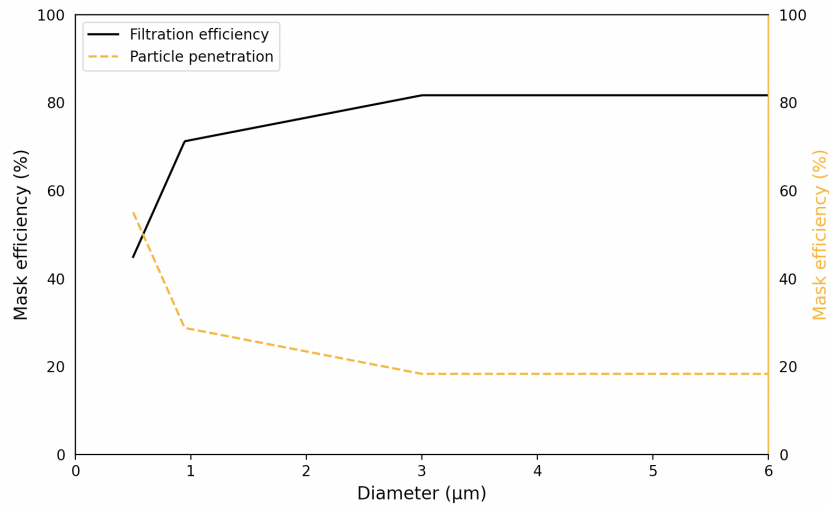


Figure S. 2: Effect of surgical mask in the outward direction. Black solid line represents the outward filtration efficiency of the mask, taking into account the leakages, based on empirical data; see Refs. [2–4]. The orange dashed line is the particle penetration yielding the relative fraction of particles that contribute to vR for different diameters. Note that, for $D \geq 3 \mu\text{m}$, the filtration efficiency is assumed constant at 82%, while it is zero below $0.5 \mu\text{m}$ due to the lack of experimental data at the time of writing.

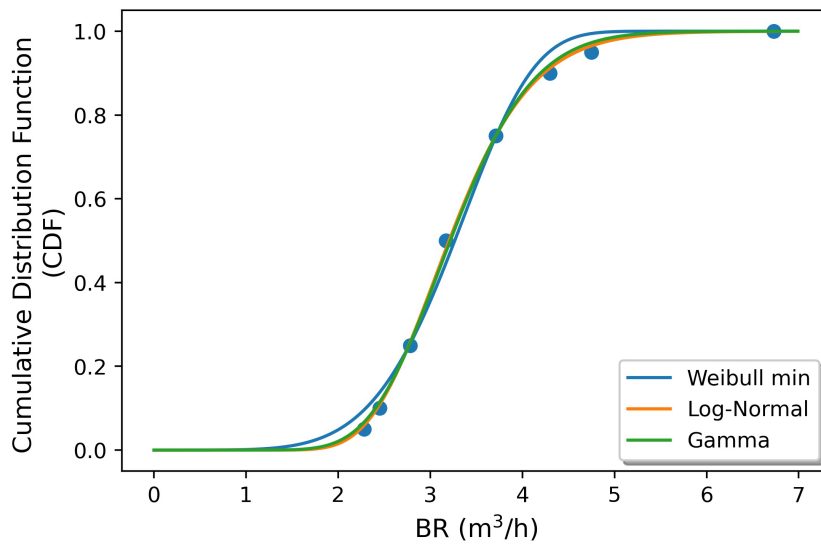


Figure S. 3: Outcomes of the fitting algorithm for the breathing rate distribution during a 'heavy exercise' activity, for three different kind of distribution functions, using the values from Supplementary Table S2. The best fit is obtained with a Log-Normal distribution: mean (SD) of $3.28 (0.72) \text{ m}^3 \text{ h}^{-1}$.

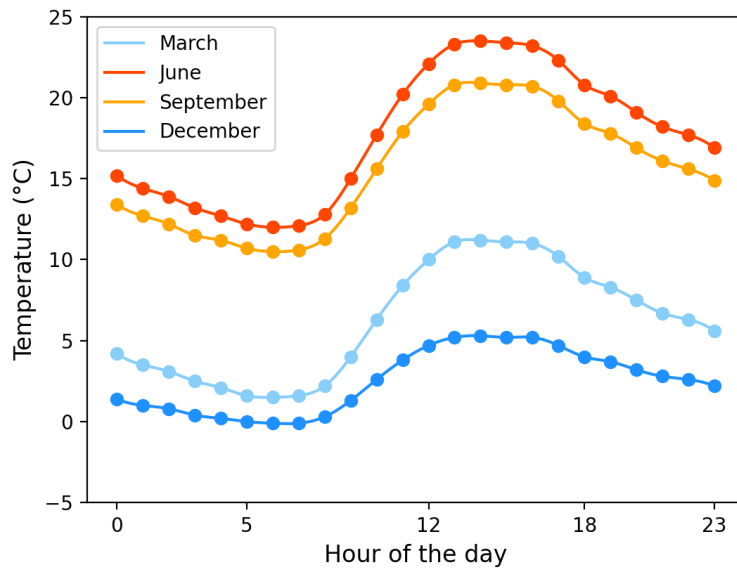


Figure S. 4: Average hourly temperature for Geneva, Switzerland. Data from hadISD [5].

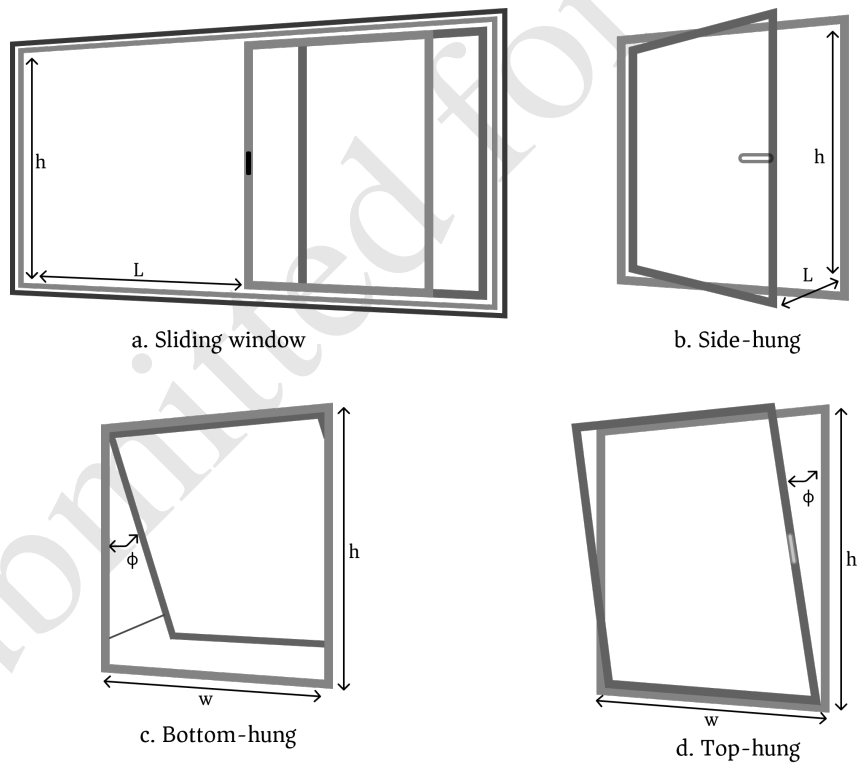


Figure S. 5: Example of window opening types for natural ventilation.

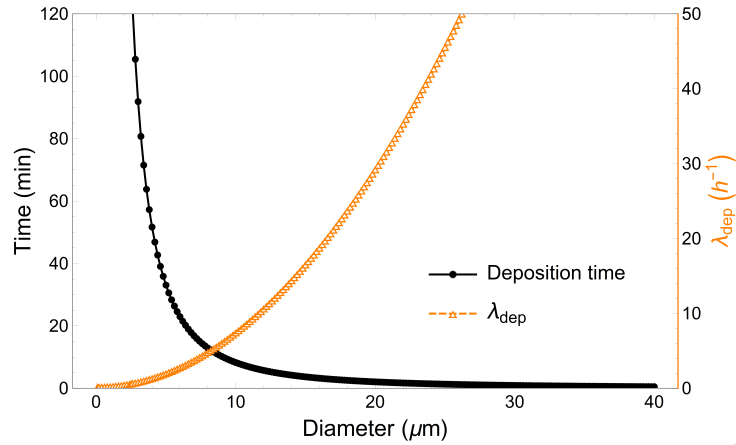


Figure S. 6: Effect of gravitational settling in standard indoor environments with typical air flow conditions. The solid line with circular markers represents the settling time of particles as a function of their size, assuming a terminal velocity at $h = 1.5$ m from the floor. The dashed line with the triangular markers represents the removal rate due to gravitational settling.

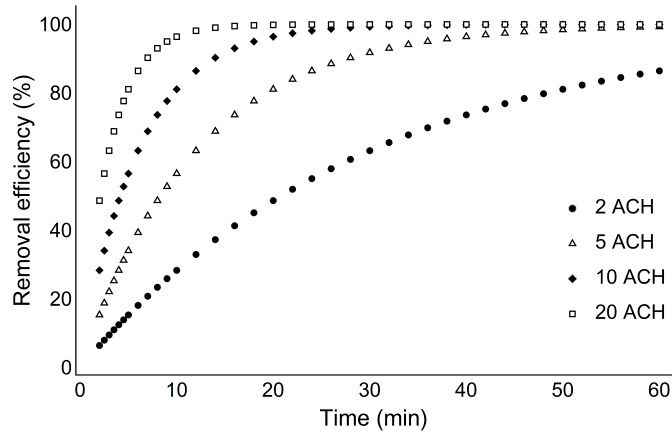


Figure S. 7: Time required to remove a fraction of the total particle load with HEPA filtration as a function of the mechanical performance of the device (in ACH). To reach a reasonable removal efficiency (e.g. 80 %) in an acceptable time frame (e.g. 20 min), we would need to select a device that would provide a removal rate (λ_{HEPA}) of about 5 ACH.

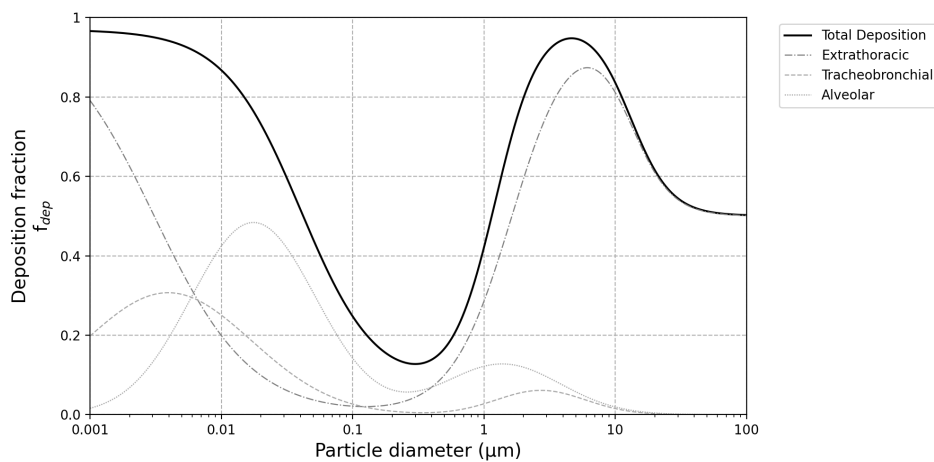
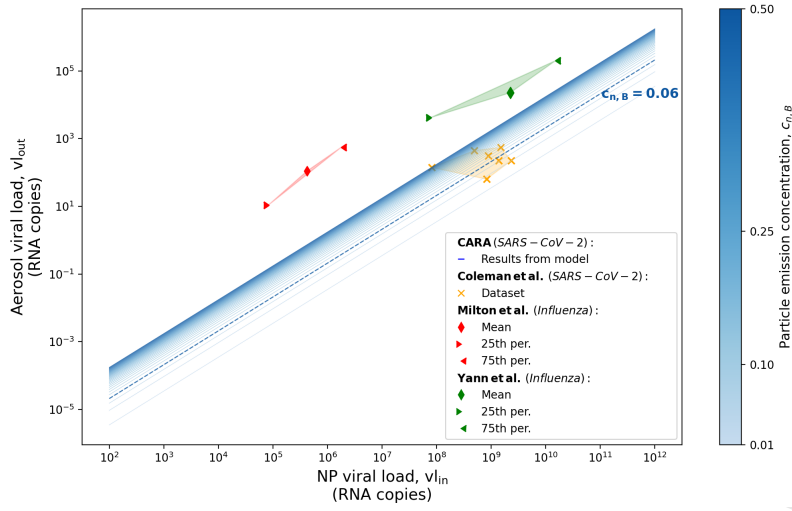
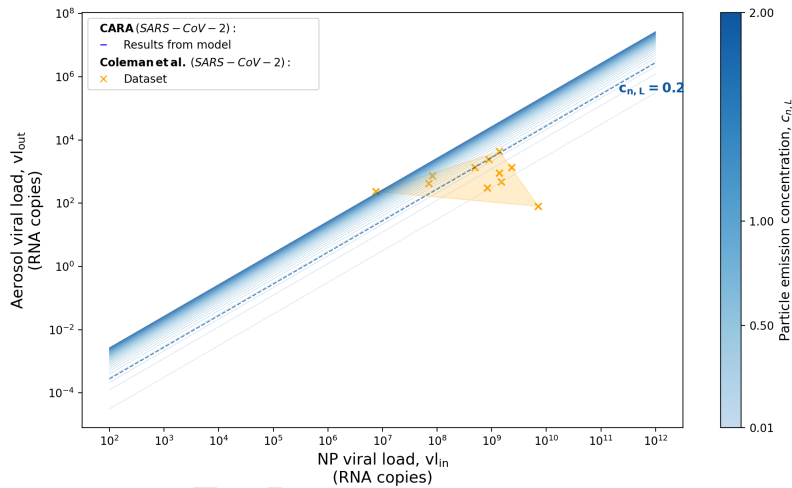


Figure S. 8: Representation of the ICRP deposition model published by Hinds [1], as a function of the particle diameter.



(a) Breathing for 30 minutes



(b) Speaking (vocalisation) for 15 minutes

Figure S. 9: Exhaled (aerosolized) RNA copies while performing respiratory and vocalisation activities, while seated, without masks, as a function of the viral load from nasopharyngeal (NP) swabs. The blue lines are the result from the model with a degraded color scale ranging the particle emission concentration $c_{n,i}$. The datasets correspond to published clinical trials for influenza [6, 7] and SARS-CoV-2 [8]. a) Results for an infected person breathing for 30 min. b) Results for an infected person under vocal speaking for 15 min. Best fit for the particle emission parameters in the BLO model: $c_{n,B} = 0.06$; $c_{n,L} = 0.2 \text{ cm}^{-3}$. For the SARS-CoV-2 data a Ct to viral load conversion factor was applied following a regression function: $y = 3.095x + 43.69$ [9].

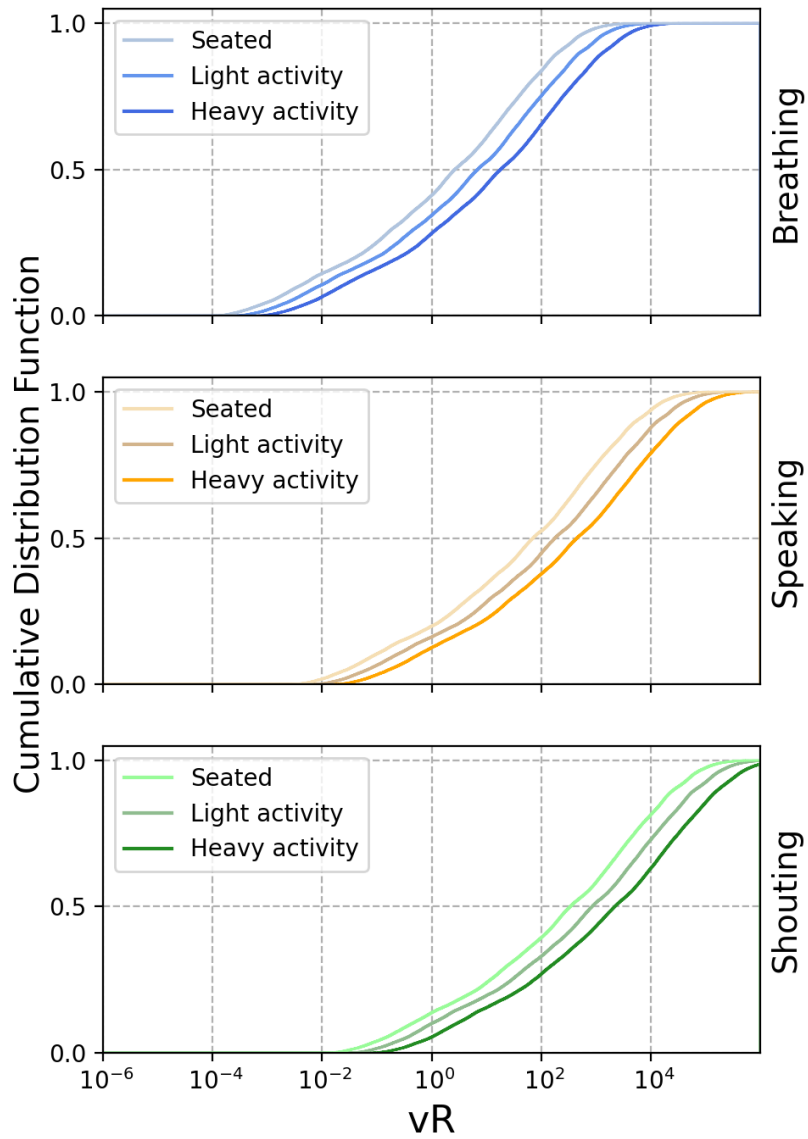


Figure S. 10: Estimation of the conditional cumulative probability of vR based on 250 000 MCS for different expiratory activities (Breathing, Speaking and Shouting - from top to bottom) and different physical activities (Seated, Light and Heavy activity). The values are without the effect of face covering ($\eta_{out} = 0$)

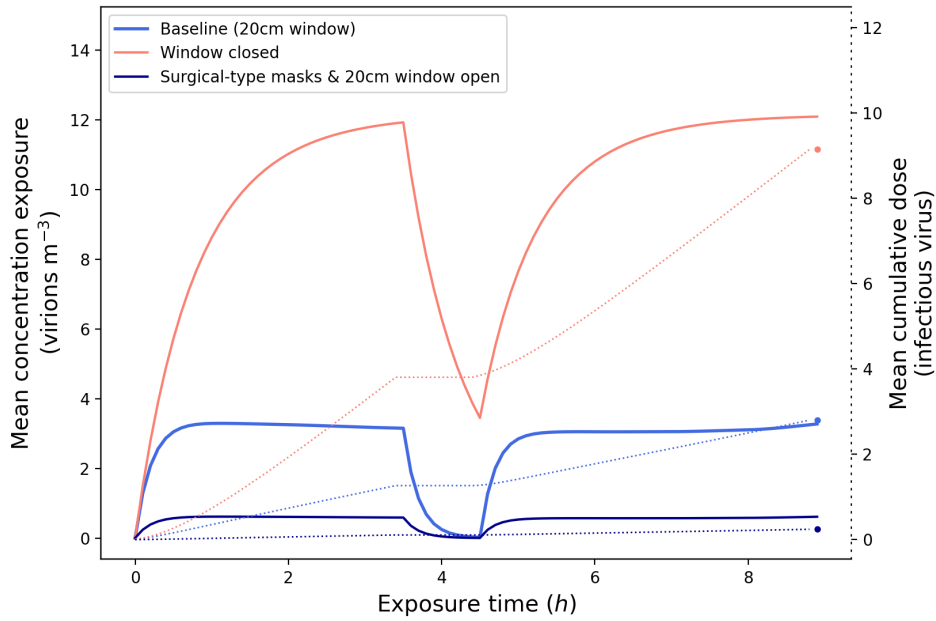


Figure S. 11: Results for the viral concentration profile over the exposure time and the cumulative absorbed dose, in the office scenario, for different combination of measures. The solid lines represent the concentration (left y-axis) and the dotted lines represent the cumulative dose (right y-axes). Time = 3.5 corresponds to a 1 hour lunch break. The horizontal section of the dotted lines correspond to the breaks, where the infected and exposed hosts leave the room and are not in contact for its duration. For visualization purposes, the confidence interval is not represented in the figure. These values can be found in Supplementary Table S4.

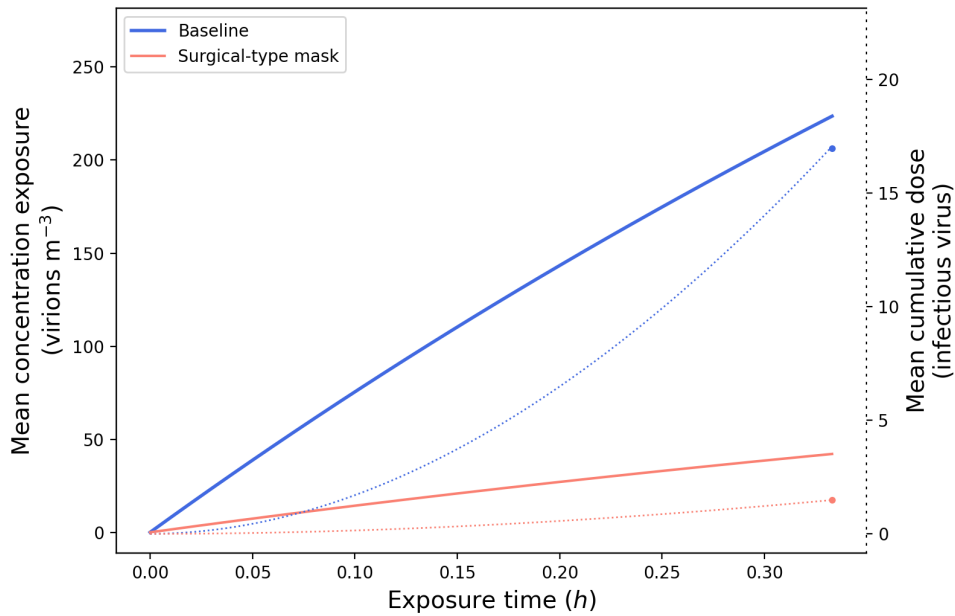


Figure S. 12: Results of the viral concentration profile over the exposure time and the cumulative absorbed dose, in the ski cabin scenario, for different combination of measures. The solid lines represent the concentration (left y-axis) and the dotted lines represent the cumulative dose (right y-axes). For visualization purposes, the confidence interval is not represented in the figure. These values can be found in Supplementary Table S4.



CARA - COVID Airborne Risk Assessment calculator

Simulation name:
Room number:

Virus data:

Room data:
 Room volume:
 Floor area:
Ceiling height:

Central heating system in use: No Yes
Location:

Ventilation data:
Ventilation type: No ventilation Mechanical Natural
Number of windows:
Height of window:
Window type: Sliding / Side-Hung Top- or Bottom-Hung
Width of window:
Opening distance:
Windows open:
 Permanently
 Periodically: /
HEPA filtration: No Yes

Event data:
Total number of occupants:
Number of infected people:

Activity type:
Exposed person(s) presence:
Start: Finish:
Infected person(s) presence:
Start: Finish:

Which month is the event?

Activity breaks:
 Input separate breaks for infected and exposed person(s)
Lunch break: No Yes
Start: Finish:
Coffee Breaks: No breaks 2 4
Duration (minutes):

Coffee breaks are spread evenly throughout the day.

Face masks:
Are masks worn when occupants are at workstations? Yes No
Type of masks used: Type 1 FFP2

Figure S. 13: Screenshot example of the CARA tool input form

S.III Tables

Table S. 1: Symbol list

Symbol	Description	Unit	Definition
D	Particle diameter	μm	
$vR(D)$	Emission rate of viruses per unit diameter	$\text{virion h}^{-1}\mu\text{m}^{-1}$	
$E_{c,j}(D)$	Volumetric particle emission concentration, for each activity j , per unit diameter	$\text{mL m}^{-3}\mu\text{m}^{-1}$	
$E_{c,j}^{\text{total}}$	Total volumetric particle emission concentration, for each activity j	mL m^{-3}	Section ??
$c_{n,i}$	Total emission concentration	cm^{-3}	
f_{amp}	Vocalisation amplification factor	-	
vl_{out}	Viral load outside the infected host	$\text{RNA copies mL}^{-1}$	
vl_{in}	Viral load inside the infected host's respiratory track		
t	Duration of the emission, exposure	h	Section ??
f_{evap}	Evaporation factor	-	
μ_{D_i}	Mean of the natural logarithm of the diameter for each mode i	$\ln \mu\text{m}$	
σ_{D_i}	Standard deviation of the natural logarithm of the diameter for each mode i	$\ln \mu\text{m}$	
$V(D)$	Volume of the particles for a given diameter D	m^3	
η_{out}	Outward mask efficiency	-	
GM	Geometric mean of the log-normal distribution for the particle diameters	μm	Section ??
GSD	Geometric standard deviation of the log-normal distribution for the particle diameters	μm	
BR_k	Breathing flow rate for a given physical activity k	$\text{m}^3 \text{h}^{-1}$	Section ??
$C(t, D)$	Viral concentration per unit diameter	$\text{virion m}^{-3}\mu\text{m}^{-1}$	Section ??
λ_{vRR}	Removal rate in the concerned room	h^{-1}	Section ??
V_r	Room volume	m^3	
N_{inf}	Number of infected hosts	-	
λ_{vRR}	Viral removal rate	h^{-1}	Section ??
λ_{ACH}	Removal rates related to ventilation		
λ_{dep}	Removal rates related to gravitational settlement		
λ_{bio}	Removal rates related to biological decay		
λ_{HEPA}	Removal rates related to filtration		

Symbol	Description	Unit	Definition
Q_{ACH}	Volumetric flow rate of fresh air supplied to the room	$m^3 h^{-1}$	Section ??
C_d	Discharge coefficient of the opening	-	
A	Area of the opening	m^2	
g	Gravitational acceleration	$m s^{-2}$	
h	Height of the opening	m	
ΔT	Indoor/outdoor air temperature difference	K	
T_{avg}	Average indoor/outdoor air temperature	K	
L	Length of the opening	m	
ϕ	Window opening angle	$^\circ$	
RH	Relative humidity	-	
v	Settling velocity of a certain particle	$m s^{-1}$	Section ??
ρ_p	Mass density of the airborne particles	$kg m^{-3}$	
ρ_{air}	Mass density of air	$kg m^{-3}$	
D_{evap}	Diameter of the desiccated particle, after evaporation	μm	
μ_{air}	Dynamic viscosity of air	$kg m^{-1} s^{-1}$	
PR ₂₀	Particle removal objective	-	Section ??
Q_{HEPA}	Effective flow rate through the filtering device	$m^3 h^{-1}$	
η_f	Filter efficiency	-	
vD^{total}	Viral dose	PFU ^a	Section ??
n	Total amount of independent exposures in the same event	-	Section ??
f_{inf}	Fraction of infectious virus	-	
r_{inf}	Viable-to-RNA virus ratio	-	
HI _{inf}	Host immunity of the infected population	-	Section ??
η_{in}	Inward mask efficiency of the PPE	-	
f_{dep}	Deposition fraction in the respiratory tract	-	Section ??
HI _{exp}	Host immunity of the exposed population	-	Section ??
$P(I)$	Probability of infection	-	
T_{voc}	Reported increase of transmissibility of a given VOC	-	
ID ₅₀	Infectious Dose	-	Section ??

^a The dose can simply be expressed as *infectious viruses* or *viable viruses*

Table S. 2: Statistical data on breathing rate (in $\text{m}^3 \text{h}^{-1}$) for ages 16-61 (with equal male/female weighting).

Activity	Mean	Quantiles (%)							
		5	10	25	50	75	90	95	100
Seated	0.51	0.43	0.44	0.47	0.50	0.54	0.58	0.61	0.80
Standing	0.57	0.49	0.50	0.53	0.56	0.60	0.64	0.67	0.86
Light Exercise	1.25	1.08	1.11	1.16	1.23	1.32	1.42	1.48	1.85
Moderate Exercise	1.78	1.30	1.38	1.53	1.72	1.97	2.26	2.46	3.64
Heavy Exercise	3.30	2.28	2.45	2.78	3.17	3.71	4.30	4.75	6.73

Table S. 3: Discharge coefficient parameters for Eq. (??) for top- or bottom-hung windows, as a function of the width over height ratio $\frac{w}{h}$ [10]

	$w/h < 0.5$	$0.5 \leq w/h < 1$	$1 \leq w/h < 2$	$w/h \geq 2$
$C_{d,max}$	0.612	0.589	0.563	0.548
$M [\text{deg}^{-1}]$	0.06	0.048	0.04	0.038

Table S. 4: Results for the vD^{total} distribution (in infectious virus) for the different scenarios and measures.

Shared office			
<i>Scenario</i>	<i>Mean</i>	<i>5th percentile</i>	<i>95th percentile</i>
Baseline	2.8	3.17E-05	14.7
W/ masks	0.2	2.56E-06	1.3
No ventilation	9.1	1.04E-04	46.7
Classroom			
<i>Scenario</i>	<i>Mean</i>	<i>5th percentile</i>	<i>95th percentile</i>
Baseline	9.6	1.07E-04	49.5
Full window open during breaks (winter)	15.7	1.76E-04	81.6
Full window open during summer	5.8	6.56E-05	30.4
HEPA filter (5 ACH)	4.5	5.12E-05	23.3
W/ masks	0.8	8.67E-06	4.2
No ventilation	21.5	2.40E-04	111.1
Ski Cabin			
<i>Scenario</i>	<i>Mean</i>	<i>5th percentile</i>	<i>95th percentile</i>
Baseline	17.0	1.83E-04	86.8
W/ masks	1.5	1.48E-05	7.4

Table S. 5: Results for the probability of infection, $P(I)$, and potential number of new (secondary) cases, N , for the different scenarios and measures.

Shared office						
<i>Scenario</i>	$P(I)$ (Mean)	$P(I)$ (5th per.)	$P(I)$ (95th per.)	<i>Occupants</i> (exposed)	N (mean)	N (95th per.)
Baseline	0.06	8E-07	0.37	3	0.18	1.10
W/ masks	0.01	7E-08	0.04		0.02	0.11
No ventilation	0.13	3E-06	0.78		0.38	2.33
Classroom						
<i>Scenario</i>	$P(I)$ (Mean)	$P(I)$ (5th per.)	$P(I)$ (95th per.)	<i>Occupants</i> (exposed)	N (mean)	N (95th per.)
Baseline	0.13	3E-06	0.78	19	2.4	14.9
Full window open during breaks (winter)	0.16	5E-06	0.92		3.1	17.5
Full window open during summer	0.10	2E-06	0.66		2.0	12.6
HEPA filter (5 ACH)	0.08	1E-06	0.52		1.6	9.9
W/ masks	0.02	2E-07	0.12		0.4	2.3
No ventilation	0.19	7E-06	0.97		3.6	18.4
Ski Cabin						
<i>Scenario</i>	$P(I)$ (Mean)	$P(I)$ (5th per.)	$P(I)$ (95th per.)	<i>Occupants</i> (exposed)	N (mean)	N (95th per.)
Baseline	0.17	5E-06	0.93	3	0.5	2.8
W/ masks	0.04	4E-07	0.21		0.1	0.6
Outbreaks (benchmark)						
<i>Scenario</i>	$P(I)$ (Mean)	$P(I)$ (5th per.)	$P(I)$ (95th per.)	<i>Occupants</i> (exposed)	N (mean)	N (95th per.)
SV Chorale ^a	0.7	0.4	0.8	60	42.5	49.2
Bus ride ^a	0.1	0.04	0.3	67	8.0	20.7

^a Assuming v_{in} is 10^9 and $5 \cdot 10^8$ copies per mL for the SV Chorale and Bus ride index hosts, respectively.

Table S. 6: Data gathered from Mikszewski et al [11] (first 3 columns) and converted to reflect the units of vR

Virus	Setting	quanta / h	virion / h (lower bound)	virion / h (upper bound)
SARS-CoV	Hospital	29	418	4176
SARS-CoV-2	Apartment	15	216	2160
SARS-CoV-2	Ship	15	216	2160
SARS-CoV-2	Bus	36	518	5184
SARS-CoV-2	Bus ride (benchmark scenario)	45	648	6480
SARS-CoV-2	Restaurant	61	878	8784
SARS-CoV-2	Bus	62	893	8928
SARS-CoV-2	School	116	1670	16704
SARS-CoV-2	Courtroom	130	1872	18720
SARS-CoV-2	Bus	133	1915	19152
SARS-CoV-2	School	139	2002	20016
SARS-CoV-2	Meeting room	139	2002	20016
SARS-CoV-2	Gym	152	2189	21888
SARS-CoV-2	Abattoir	232	3341	33408
SARS-CoV-2	Call Center	683	9835	98352
SARS-CoV-2	S V Chorale (benchmark scenario)	970	13968	139680
SARS-CoV-2	Choir	4213	60667	606672
Measles	Classroom	18	259	2592
Measles	Classroom	600	8640	86400
Measles	Classroom	2765	39816	398160
Measles	Office	8640	124416	1244160
Influenza	Quarantine rooms	0.11	2	16
Influenza	Clinical tria (ferrets)	7.95	114	1145
Influenza	Airplane	79	1138	11376
Rhinovirus	Clinical trial (humans, leisure)	3.1	45	446

Bibliography

- [1] W. C. Hinds, *Aerosol technology: properties, behavior, and measurement of airborne particles*, pp. 233 – 259. New York: Wiley, 1999.
- [2] J. Pan, C. Harb, W. Leng, and L. C. Marr, “Inward and outward effectiveness of cloth masks, a surgical mask, and a face shield”, *Aerosol Science and Technology*, pp. 1–16, Feb 2021. doi.org/10.1080/02786826.2021.1890687.
- [3] D. J. Huang and V. Huang, “Evaluation of the Efficiency of Medical Masks and the Creation of New Medical Masks”, *Journal of International Medical Research*, vol. 35, no. 2, pp. 213–223, 2007. doi.org/10.1177/147323000703500205.

- [4] S. Asadi, C. D. Cappa, S. Barreda, *et al.*, “Efficacy of masks and face coverings in controlling outward aerosol particle emission from expiratory activities”, *Scientific reports*, vol. 10, no. 1, pp. 1–13, 2020. doi.org/10.1038/s41598-020-72798-7.
- [5] R. J. H. Dunn, “HadISD version 3: monthly updates”, *Hadley Centre Technical Note*, 2019.
- [6] D. K. Milton, M. P. Fabian, B. J. Cowling, M. L. Grantham, and J. J. McDevitt, “Influenza Virus Aerosols in Human Exhaled Breath: Particle Size, Culturability, and Effect of Surgical Masks”, *PLOS Pathogens*, vol. 9, p. e1003205, Mar 2013. doi.org/10.1371/journal.ppat.1003205.
- [7] J. Yan, M. Grantham, J. Pantelic, P. J. Bueno de Mesquita, B. Albert, F. Liu, S. Ehrman, D. K. Milton, and E. M. I. T. Consortium, “Infectious virus in exhaled breath of symptomatic seasonal influenza cases from a college community”, *Proceedings of the National Academy of Sciences*, vol. 115, p. 1081, Jan 2018. doi.org/10.1073/pnas.1716561115.
- [8] K. K. Coleman, D. J. W. Tay, K. Sen Tan, S. W. X. Ong, T. T. Son, M. H. Koh, Y. Q. Chin, H. Nasir, T. M. Mak, J. J. H. Chu, *et al.*, “Viral Load of SARS-CoV-2 in Respiratory Aerosols Emitted by COVID-19 Patients while Breathing, Talking, and Singing”, *Clinical Infectious Diseases*, Aug 2021. doi.org/10.1093/cid/ciab691.
- [9] M. S. Han, J.-H. Byun, Y. Cho, and J. H. Rim, “RT-PCR for SARS-CoV-2: quantitative versus qualitative”, *The Lancet Infectious Diseases*, vol. 21, p. 165, Feb 2021. doi.org/10.1016/S1473-3099(20)30424-2.
- [10] R. Daniels, “BB 101: Ventilation, thermal comfort and indoor air quality 2018”, report, UK government - Education and Skills Funding Agency, London, 2018. www.gov.uk/government/publications/building-bulletin-101-ventilation-for-school-buildings.
- [11] A. Mikszewski, L. Stabile, G. Buonanno, and L. Morawska, “The airborne contagiousness of respiratory viruses: A comparative analysis and implications for mitigation”, *Geoscience Frontiers*, p. 101285, Aug 2021. doi.org/10.1016/j.gsf.2021.101285.